14

BNWL-1845-26
UC-23

Pacific Northwest Laboratory Monthly Report to the Nuclear Research and Applications Division for July 1976

H. T. Fullam

August 1976

Prepared for the Energy Research and Development Administration under Contract E(45-1)-1830

Battelle
Pacific Northwest Laboratories

BNWL-1845-26

PACIFIC NORTHWEST LABORATORY
operated by
BATTELLE
for the
ENERGY RESEARCH AND DEVELOPMENT ADMINISTRATION
Under Contract *E(45-1)-1830*

Printed in the United States of America
Available from
National Technical Information Service
U.S. Department of Commerce
5285 Port Royal Road
Springfield, Virginia 22151
Rie: Printed Copy $5.00; Microfiche $2.25

BNWL-1845-26
UC-23

PACIFIC NORTHWEST LABORATORY MONTHLY REPORT TO THE NUCLEAR RESEARCH AND APPLICATIONS DIVISION FOR JULY 1976

H. T. Fullam

August 1976

Battelle
Pacific Northwest Laboratories
Richland, Washington 99352

CONTENTS

LIST OF FIGURES

PACIFIC NORTHWEST LABORATORY
MONTHLY REPORT TO THE
NUCLEAR RESEARCH AND APPLICATIONS DIVISION
FOR JULY 1976

STRONTIUM HEAT SOURCE DEVELOPMENT PROGRAM

At Hanford, strontium is separated from the high-level waste, then converted to the fluoride, and doubly encapsulated in small, high-integrity containers for subsequent long-term storage. The fluoride conversion, encapsulation and storage take place in the Waste Encapsulation and Storage Facilities (WESF). This encapsulated strontium fluoride represents an economical source of ^{90}Sr if the WESF capsule can be licensed for heat source applications under anticipated use conditions. The objectives of this program are to obtain the data needed to license $^{90}SrF_2$ heat sources and specifically the WESF $^{90}SrF_2$ capsules. The information needed for licensing can be divided into three general areas:

1. *Long-term SrF_2 compatibility data.*
2. *Chemical and physical property data on $^{90}SrF_2$.*
3. *Capsule property data such as external corrosion resistance, crush strength, etc.*

The current program is designed to provide the required information.

LONG-TERM COMPATIBILITY TESTS

The long-term compatibility tests are continuing as scheduled. The 36 radioactive test specimens from the 1000-hr tests are being analyzed at the Oak Ridge National Laboratory. Metallographic examination of the specimens is approximately 60% completed and electron microprobe analyses of selected specimens will start in August and the results will be reported when all of the data are available.

Compatibility testing of the two full-size WESF capsules is continuing. After several weeks delay because of the strike, the taking of capsule surface temperatures was resumed at the end of July. The latest measurements

indicate a maximum $^{90}SrF_2$-metal interface temperature of 825°C in one capsule and 821°C in the second. A temperature gradient across the length of the capsule of approximately 40°C was observed with each capsule.

The thermal gradient test with Hastelloy C-276-WESF-grade SrF_2 is continuing. No fluctuations in the capsule surface temperatures have been observed; and the temperature gradient along the capsule length of 560°C (920°C to 360°C) is being maintained as planned.

ADDITIONAL SHORT-TERM COMPATIBILITY TESTS

Short-term compatibility tests are underway to evaluate potential containment materials not covered in the initial short-term tests. Thirty-two materials, including Haynes Alloy 25, Hastelloy C-276 and TZM as reference specimens, are being tested at 800°C for 1500 and 4400 hr. Non-radioactive SrF_2, having approximately the same composition as WESF $^{90}SrF_2$, is being used for the tests. Testing and metallographic examination of the 1500-hr test couples have been completed; and estimates of metal attack based on photomicrographs of the test specimens are presented in Table 1. These estimates are divided into two classifications: chemical attack and changes in metal microstructure. Chemical attack is defined as those attack mechanisms which can be directly attributed to reactions involving SrF_2 and include such phenomena as surface dissolution, pitting, grain boundary attack and subsurface void formation. Microstructural changes are those affected areas where the metal morphology differs from that of control specimens. These changes can include the disappearance of normal alloy precipitates, the appearance of abnormal precipitates or marked changes in grain size. Since the microstructural changes do not occur in control specimens they can be attributed to SrF_2 attack.

Most of the nickel- and cobalt-base alloys suffered both types of attack. In the case of the refractory and noble metal alloys the attack consisted principally of chemical attack and there were few indications of microstructural changes (in some cases it was difficult to evaluate possible microstructural changes because of the extensive chemical attack?

TABLE 1. Metal Attack in Test Specimens Exposed to Nonradioactive SrF_2 at 800°C for 1500 hr

Material	Depth of Metal Affected, mils: Chemical Attack	Depth of Metal Affected, mils: Change in Microstructure
Hastelloy C-276[a]	3	7
Haynes Alloy 25[a]	2	3
TZM[a]	1	0
Hastelloy C-4	5	12
Hastelloy B	4	15
Hastelloy B-2	10	18
Hastelloy S	7	15
Haynes Alloy 556	5	6
Inconel 617	7	14
Inconel 671	15	25
Incoloy 800	8	0
Rene 41	10	14
Udimet 700	>25	0
Monel 400	5	8
Nickel 200	7	10
Ingot Iron	3	0
Ductile Cast Iron	CR	CR[c]
316L SS	6	0
JS 777	6	7
Copper	>25	0
Titanium	>25	(b)
Hafnal loy 2525	>25	-
Molybdenum	2	0
Niobium	3	2
Ta-10% W	10	0
Mo-50% Re	2	
W-26% Re	2	0
Rhenium	<1	0
Iridium	0	0
Ir-0.3% W	0	0
Platinum	>25	-
Gold	>15	

(a) Tested as reference specimen
(b) - could not be determined because of extensive chemical attack
(c) CR-complete reaction

Of the various nickel- and cobalt-base alloys tested, none appeared as resistant to SrF_2 attack as the Haynes Alloy 25 and Hastelloy C-276 which were evaluated in the initial short-term compatibility tests. Several refractory metal and noble metal alloys appear to be quite resistant to SrF_2 attack and may offer potential as a clad material for $^{90}SrF_2$ in special applications. The types of attack observed in the various couples are discussed in the following sections.

Hastelloy C-276 - SrF_2

Attack of the Hastelloy C-276 was similar to that observed in the initial short-term compatibility tests with $^{90}SrF_2$. Chemical attack consisted of general surface dissolution with some grain boundary attack and subsurface void formation (Figure 1-a). Microstructural changes consisted of a surface layer several mils thick containing a heavy concentration of abnormal precipitates and an adjacent inner layer where normal precipitates were largely depleted.

Haynes Alloy 25 - SrF_2

Attack was similar to that found in the initial short-term tests. Chemical attack consisted primarily of grain boundary attack and pitting with some surface dissolution (Figure 1-b). Depletion of normal alloy precipitates (Laves phase M_6C carbides) was apparent in a thin surface layer.

TZM - SrF_2

Very slight chemical attack with formation of a thin reaction layer at the specimen surface (Figure 1-c), some pitting and grain boundary attack. No apparent changes in the microstructure.

Hastelloy C-4 - SrF_2

Extensive chemical attack consisting of a general surface reaction with formation of an adherent reaction layer at the surface. Only slight indication of grain boundary attack. Etching of the test specimen resulted in leaching of part of the reaction layer (Figure 1-d). Microstructural

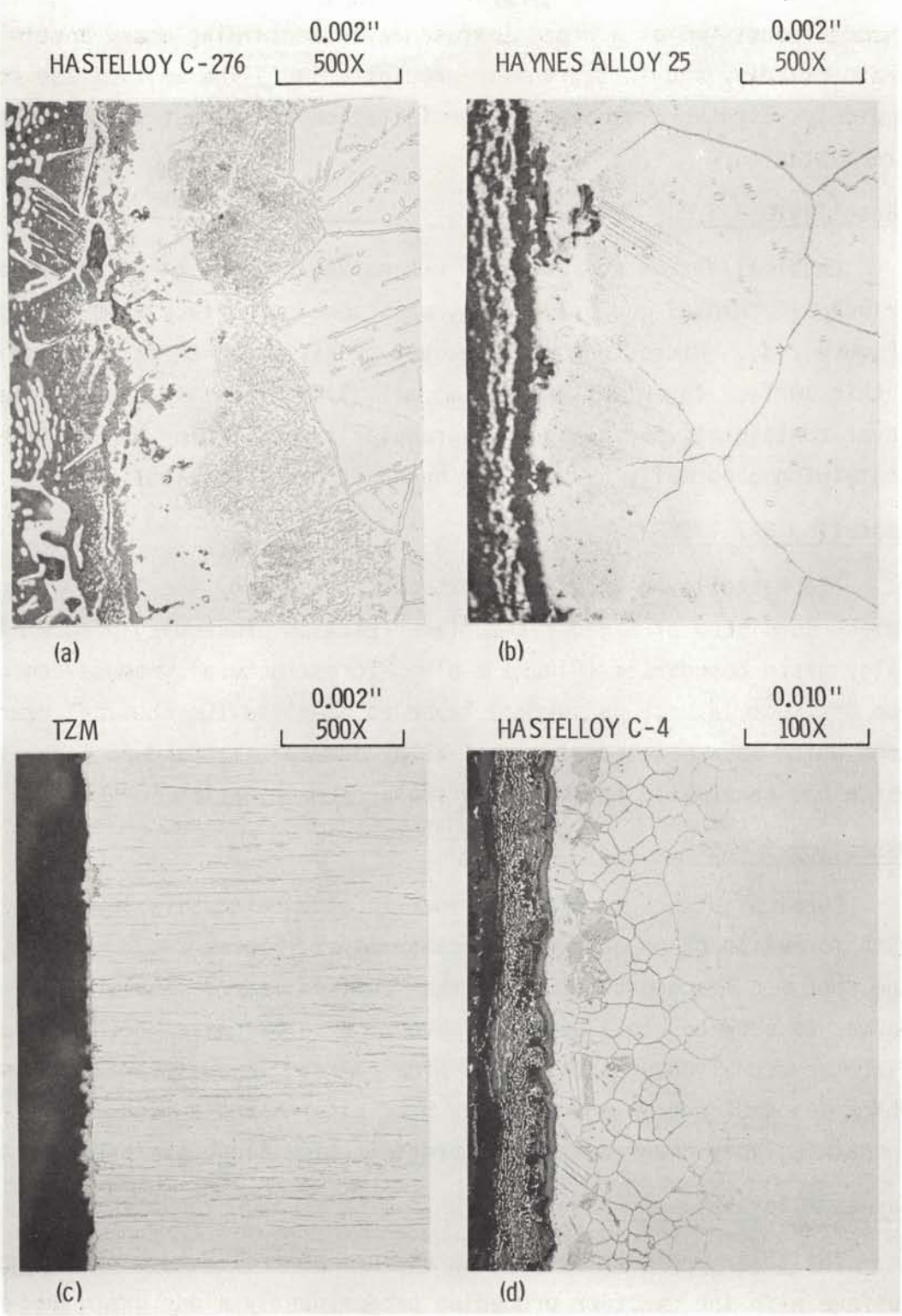

FIGURE 1. Test Specimens Exposed to SrF_2 at 800°C for 1500 hr

changes consisted of a broad surface layer containing heavy continuous grain boundary and intragranular precipitation. The bulk of the specimen had only slight grain boundary precipitation and almost no intragranular precipitation.

Hastelloy B - SrF_2

Chemical attack consisted of extensive leaching of alloy components, principally nickel and molybdenum, with some subsurface void formation (Figure 2-a). Microstructural changes consisted of three distinct layers: a thin surface layer depleted of normal alloy precipitates; an intermediate layer containing very heavy intragranular precipitation and an inner layer containing abnormally heavy grain boundary precipitation.

Hastelloy B-2 - SrF_2

The Hastelloy B-2 suffered extensive attack by the SrF_2. Chemical attack consisted of a general surface reaction proceeding predominantly alloy grain boundaries (Figure 2-b). Microstructural changes consisted of two distinct layers: a surface layer adjacent to'the chemical reaction zone which was depleted of normal alloy precipitates and an inner layer which had abnormally heavy intragranular precipitation.

Hastelloy S - SrF_2

Chemical attack consisted primarily of an extensive layered attack with formation of an adherent reaction layer (Figure 2-c). Etching of the. specimen leached out much of the reaction layer. Subsurface void formation occurred to a depth of several mils below the reaction layer. Microstructural changes consisted of a surface layer several mils thick which was depleted in normal alloy precipitates and a much wider layer containing very heavy continuous precipitation along grain boundaries.

Haynes Alloy 556 - SrF_2

The test specimens suffered a uniform general attack of the metal surface with the reaction proceding predominantly along grain boundaries. An adherent reaction layer formed on the surface which leached away when

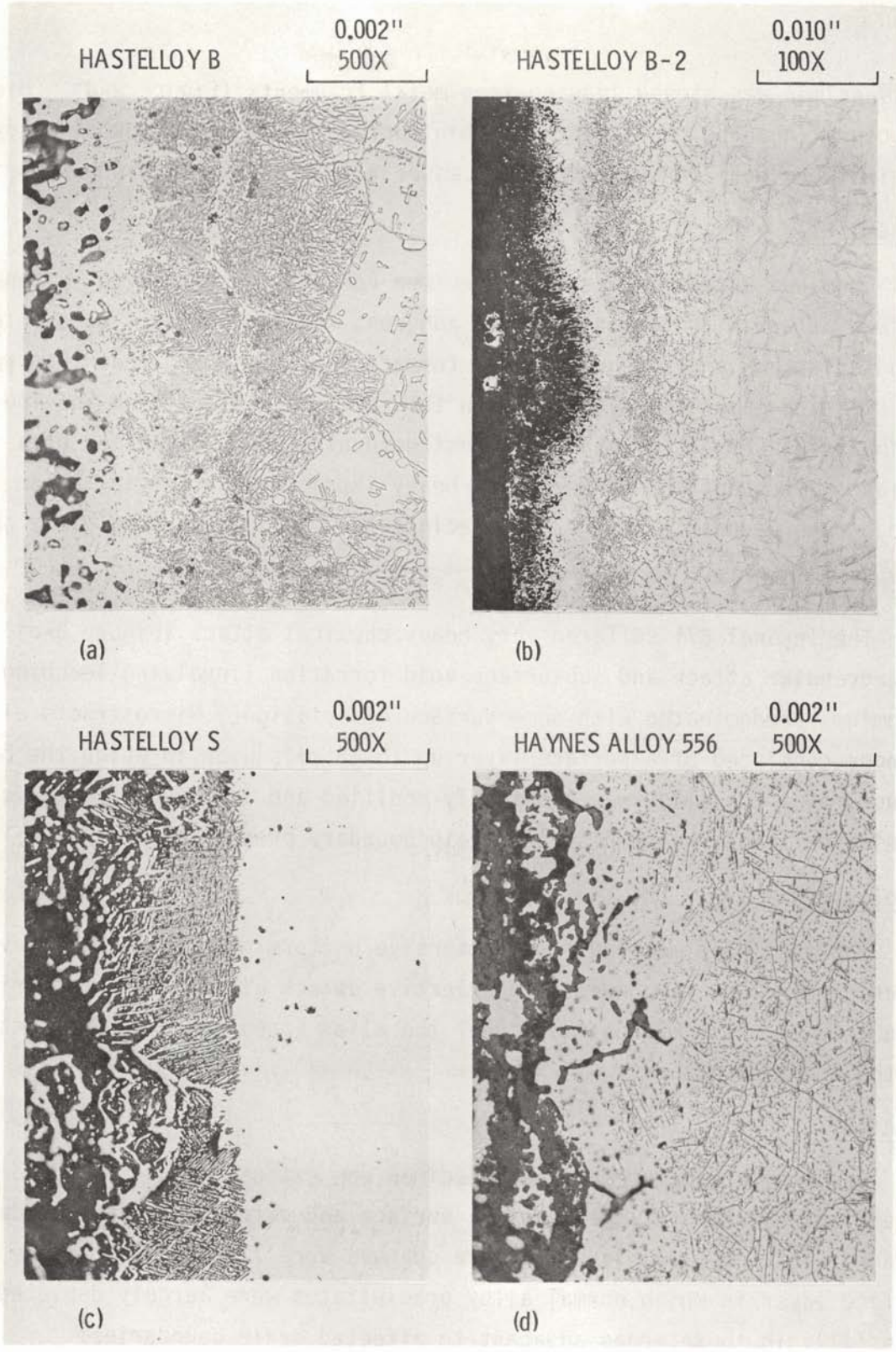

FIGURE 2. Nickel Alloy Specimens Exposed to SrF_2 at 800°C for 1500 hr

the specimen was etched leaving free metal fragments (Figure 2-d). Microstructural changes consisted of a thin surface layer where normal alloy precipitates were largely depleted, especially along the grain boundaries.

Inconel 617 - SrF_2

Chemical attack of the test specimen consisted primarily of a general surface attack with formation of an adherent reaction layer. Some intergranular attack and subsurface void formation was also apparent (Figure 3-a). The reaction layer leached away when the specimens were etched leaving stringers of unreacted metal. Microstructural changes consisted of a surface layer containing abnormally heavy intragranular precipitation, except along grain boundaries where the precipitates were almost completely absent.

Inconel 671 - SrF_2

The Inconel 671 suffered very heavy chemical attack (Figure 3-b). Intergranular attack and subsurface void formation (involving leaching of chromium) predominated with some surface dissolution. Microstructural changes consisted of a surface layer up to 15 mils wide in which the basic structure of the alloy was apparently modified and an adjacent layer containing extremely heavy discrete grain boundary precipitates.

Incoloy 800 - SrF_2

The test specimens suffered extensive uniform chemical attack involving leaching of alloy components and selective attack along grain boundaries (Figure 3-c). The microstructure of the alloy appeared to be uneffected by the chemical attack.

Rene 41 - SrF_2

Chemical attack of the test specimen was extensive and consisted of general dissolution of the specimen surface and extensive grain boundary attack (Figure 3-d). Microstructure changes were limited to a single surface layer in which normal alloy precipitates were largely depleted - especially in those areas adjacent to affected grain boundaries.

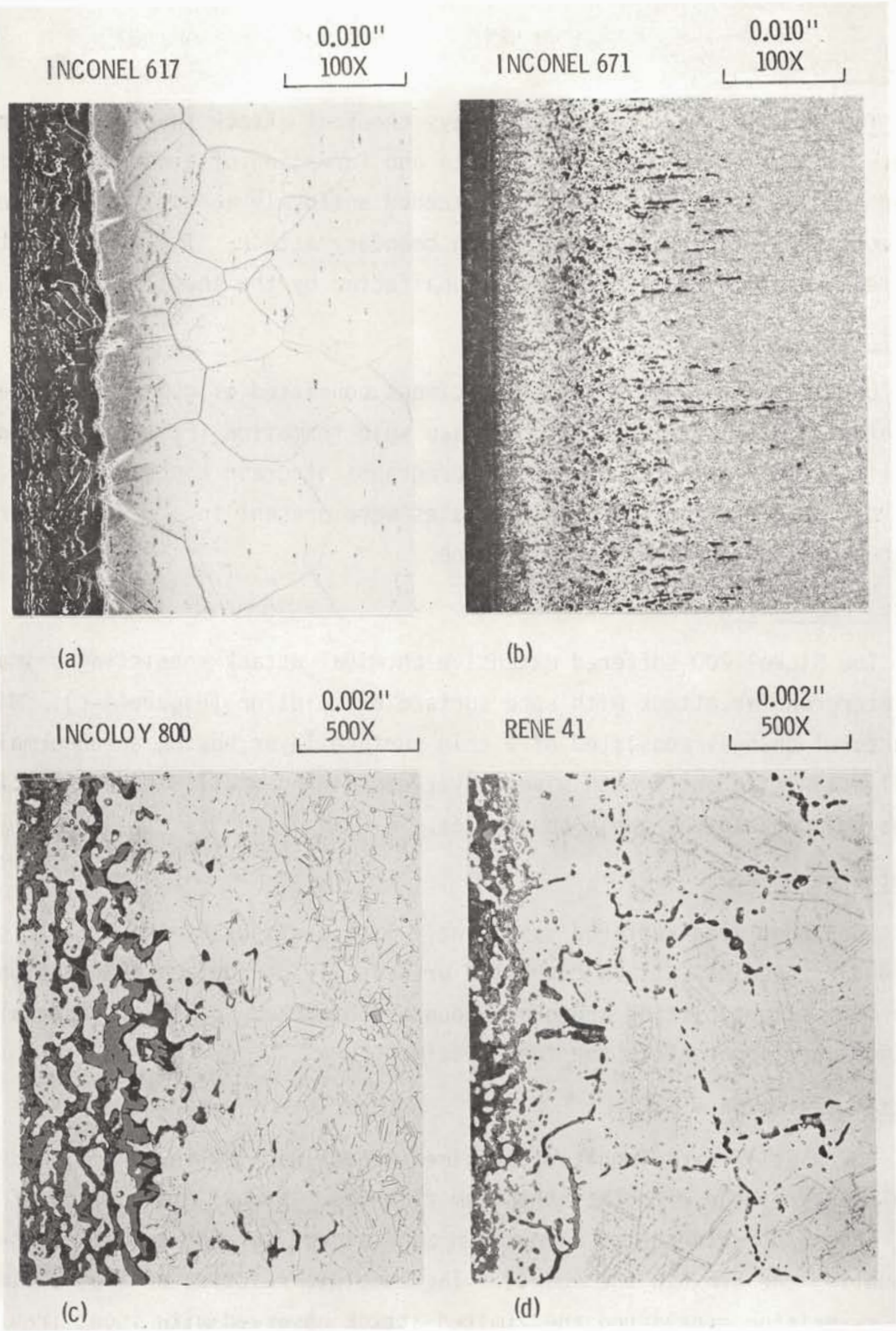

FIGURE 3. Photomicrographs of Specimens Exposed to SrF_2 at 800°C for 1500 hr

Udimet 700 - SrF_2

The Udimet 700 suffered very heavy chemical attack involving a general layered attack of the specimen surface and formation of a adherent reaction layer (Figure 4-a). The reaction proceded uniformly across the specimen surface with little evidence of grain boundary attack. The microstructure outside the reaction layer appeared unaffected by the chemical attack.

Monel 400 - SrF_2

Chemical attack of the test specimens consisted of general surface dissolution with pitting and subsurface void formation (Figure 4). There was little indication in the photomicrographs of grain boundary attack. Fine discrete intragranular precipitates were present in a narrow layer adjacent to the chemical reaction zone.

Nickel 200 - SrF_2

The Nickel 200 suffered extensive chemical attack sonsisting primarily of intergranular attack with some surface dissolution (Figure 4-c). Microstructural changes consisted of a thin surface layer having an abnormally small grain size and a much wider layer containing small discrete precipitates adjacent to the grain boundaries.

Ingot Iron - SrF_2

The ingot iron suffered suprisingly little attack by the SrF_2 (Figure 4-d). Chemical attack consisted principally of surface dissolution with some slight pitting and grain boundary attack. No microstructural changes were apparent in the test specimen.

Ductile Cast Iron - SrF_2

The ductile cast iron test specimen, which was 1/8 in. thick, had completely reacted with the strontium fluoride. Visual examination of the SrF_2 showed no evidence of a reaction zone except for the complete discoloration the SrF_2 in the couple. The complete reaction of the specimens very surprising considered the limited attack observed with ingot iron. The test will be repeated using a different source of ductile cast iron.

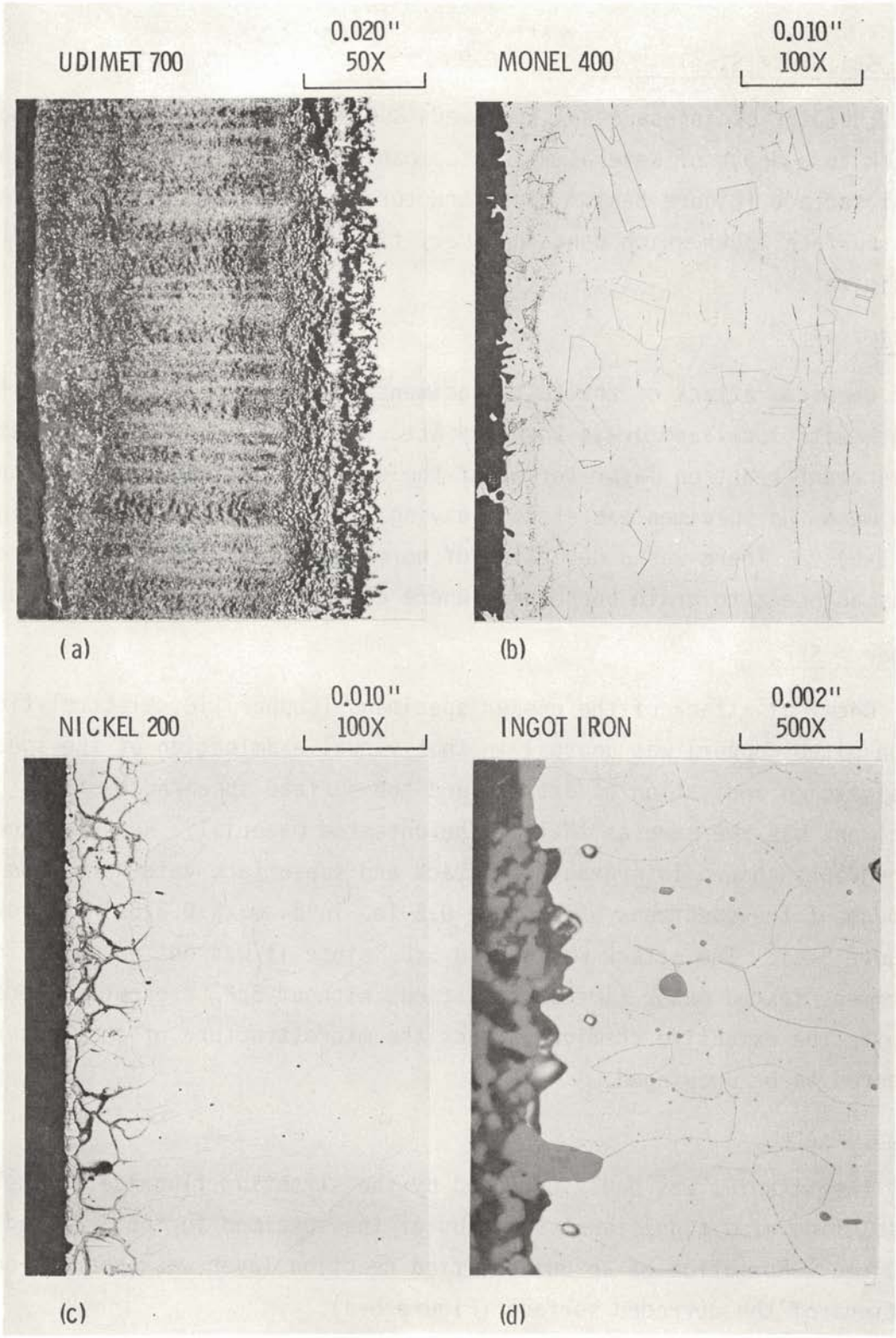

FIGURE 4. Photomicrograph of Specimens Contacted with SrF_2 at 800°C for 1500 hr

316L Stainless Steel - SrF_2

The 316L stainless steel specimens suffered localized grain boundary attack to a depth of several mils accompanied by general dissolution of the metal surface (Figure 5-a). Microstructural changes were limited to a thin surface layer which contained very fine discrete intragranular precipitates.

JS-777-SrF_2

Chemical attack of the test specimens consisted of a general surface attack with localized grain boundary attack and subsurface void formation. An adherent reaction layer formed at the specimen surface, which leached away when the specimen was etched leaving fragments of free metal (Figure 5-b). There was a depletion of normal alloy precipitates in the areas adjacent to grain boundaries where chemical attack had occurred.

Copper - SrF_2

Chemical attack of the copper specimens (Copper 110, electrolytic tough pitch copper) was unusual in that visual examination of the specimens gave no indication of attack, and the surface appearance of the specimens was the same as that of the untested material. However, the micrographs showed intergranular attack and subsurface void formation throughout the specimens which were 0.5 in. in diam. x 0.375 in. thick (Figure 5-c). The attack was due to SrF_2 since it was not observed in specimens tested under similar conditions without SrF_2 present (Figure 5-d). Despite the extensive chemical attack the microstructure of the copper appeared to be unchanged.

Titanium-SrF_2

The titanium was badly corroded by the strontium fluoride. Complete dissolution of a significant fraction of the specimen in the SrF_2 had occurred. Formation of an unidentified reaction layer was apparent on portions of the corroded surface (Figure 6-a).

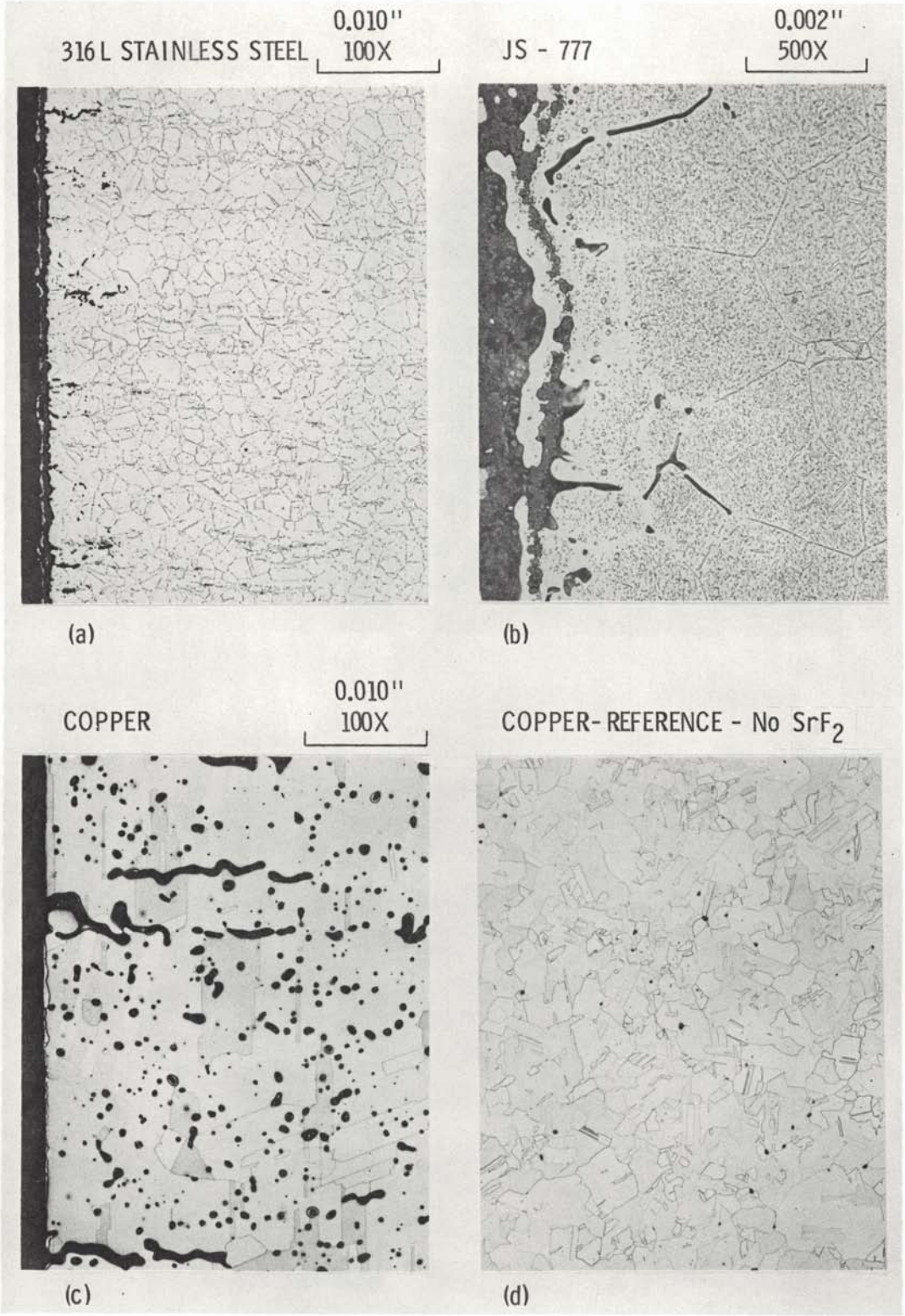

FIGURE 5. Specimens Exposed to SrF_2 at 800°C for 1500 hr

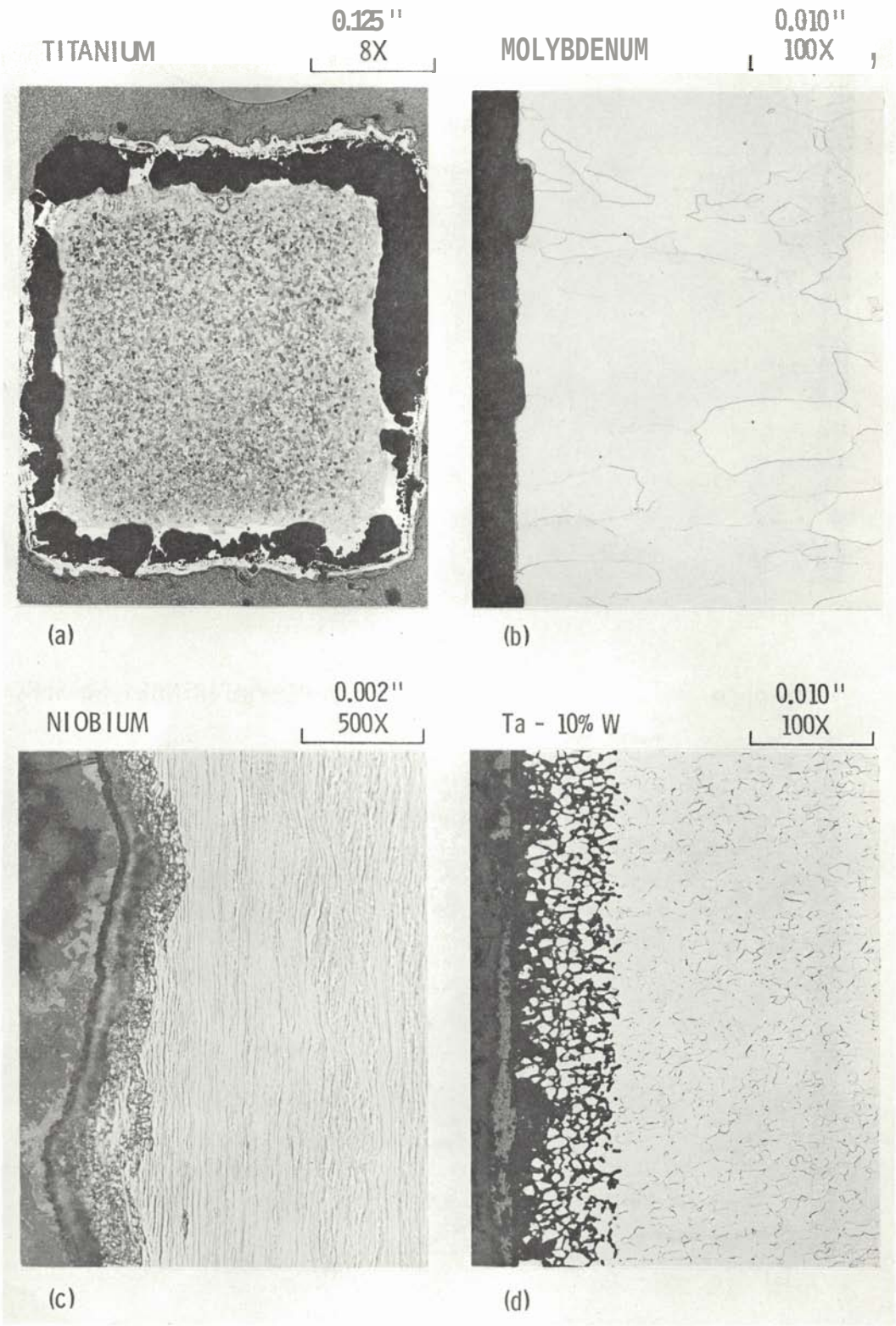

FIGURE 6. Metal Samples Contacted with SrF_2 at 800°C for 1500 hr

Hafnalloy 2525

The Hafnalloy 2525 specimens were almost completely consumed by the strontium fluoride. Examination of the SrF_2 showed small fragments of the specimen dispersed in the SrF_2.

Molybdenum - SrF_2

Chemical attack of the molybdenum specimen was greater than expected considering the resistance of TZM to SrF_2 attack. General surface dissolution predominated with pitting and some grain boundary attack (Figure 6-b). Formation of a reaction layer was apparent on portions of the specimen surface. No microstructural changes were apparent in the specimens.

Niobium - SrF_2

Chemical attack of the niobium specimen consisted of a general surface attack with formation of an adherent reaction layer (Figure 6-c). No microstructural changes were observed in the test specimens.

Ta-10%W - SrF_2

The Ta-10%W suffered extensive chemical attack by the SrF_2. The attack was uniform across the exposed surface; and appeared to proceed along grain boundaries leaving individual metal grains in an adherent reaction layer (Figure 6-d). The reaction layer leached away when the specimen was etched. The microstructure of the alloy was unaffected by the SrF_2.

Mo-50% Re - SrF_2

Chemical attack of the Mo-50% Re samples consisted of a general layered attack with formation of an adherent reaction layer. Some grain boundary attack proceeded the layer attack. Etching of the test specimen dissolved the reaction layer leaving small fragments of unreacted metal (Figure 7-a).

W-26% Re - SrF_2

The W-26% Re specimens suffered a general surface attack with formation of an adherent reaction layer. Etching of the specimen dissolved most of the reaction layer leaving some unreacted metal fragments (Figure 7-b). The microstructure of the alloy appeared to be unaffected by the SrF_2.

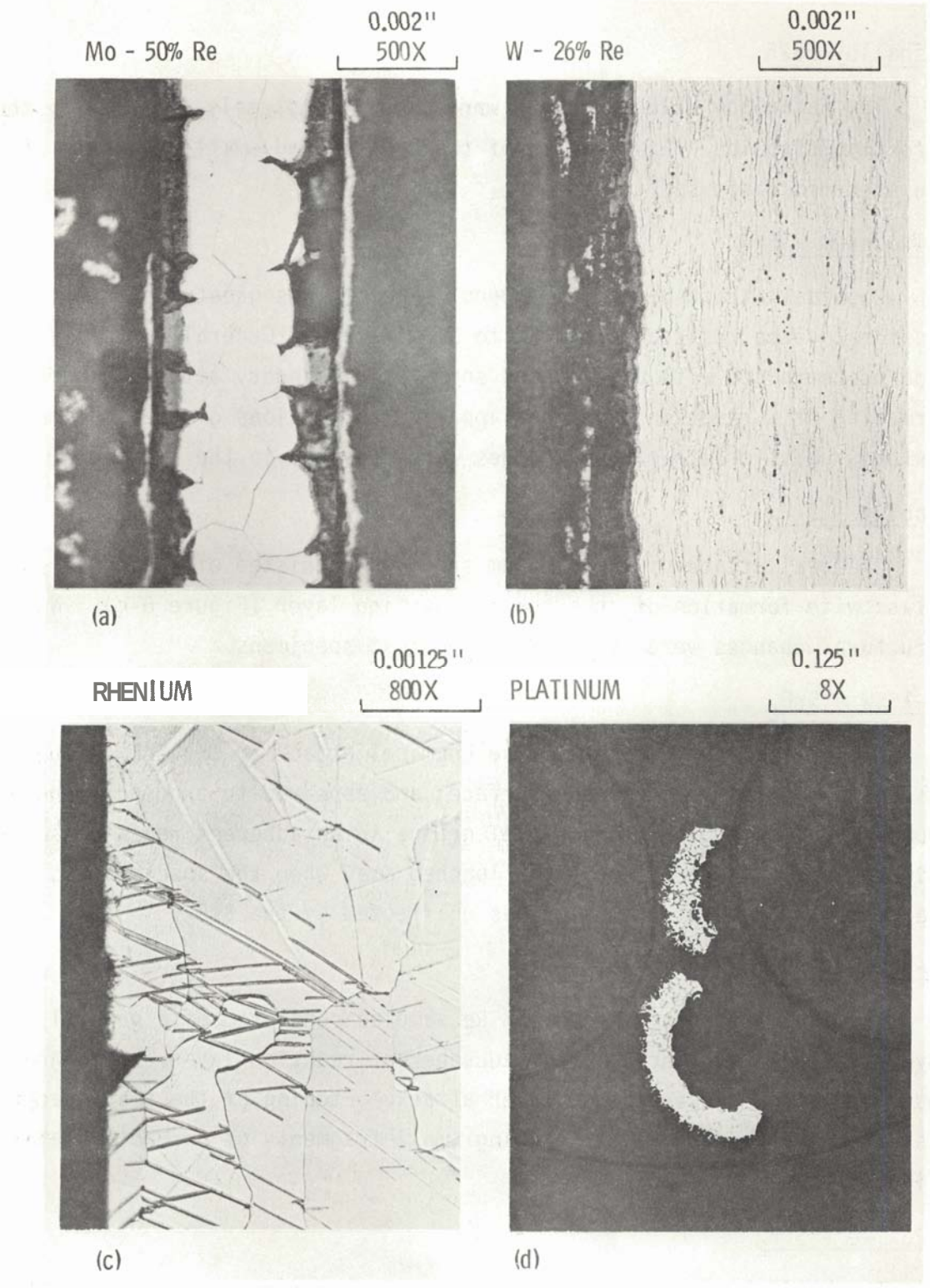

FIGURE 7. Metal Specimens Exposed to SrF_2 at 800°C for 1500 hr

Rhenium - SrF_2

Rhenium was almost unaffected by the SrF_2 (Figure 7-c). One specimen exhibited what may be slight pitting, but the observed effect may be due to a flaw in the original test specimen.

Iridium - SrF_2

The iridium was completely unreactive with the SrF_2 and there was no evidence of fluoride attack.

Ir - 0.3% W - SrF_2

The alloy was completely unreactive with the SrF_2 and there was no evidence of SrF_2 attack.

Platinum - SrF_2

The platinum specimens, which were sections of platinum tubing, were partially consumed by the SrF_2. Recovered segments of the specimens are shown in Figure 7-d. Attack apparently proceeded along grain boundaries leaving fragments of unaffected metal. The reacted platinum apparently dissolved in the SrF_2 as there was no indication of a reaction layer.

Gold - SrF_2

The gold was partially consumed by the SrF_2. The test specimens were approximately 15 mils thick and were completely corroded through at various spots, while other areas appeared to be unaffected (Figure 8).

HASTELLOY C-4 CORROSION RESISTANCE

Tests are underway to measure the seawater corrosion resistance and oxidation resistance of Hastelloy C-4. The initial tests utilize the alloy in the solution heat treated form as received from the vendor. Future tests will use specimens which have been aged at various temperatures. Tests with welded specimens are also planned.

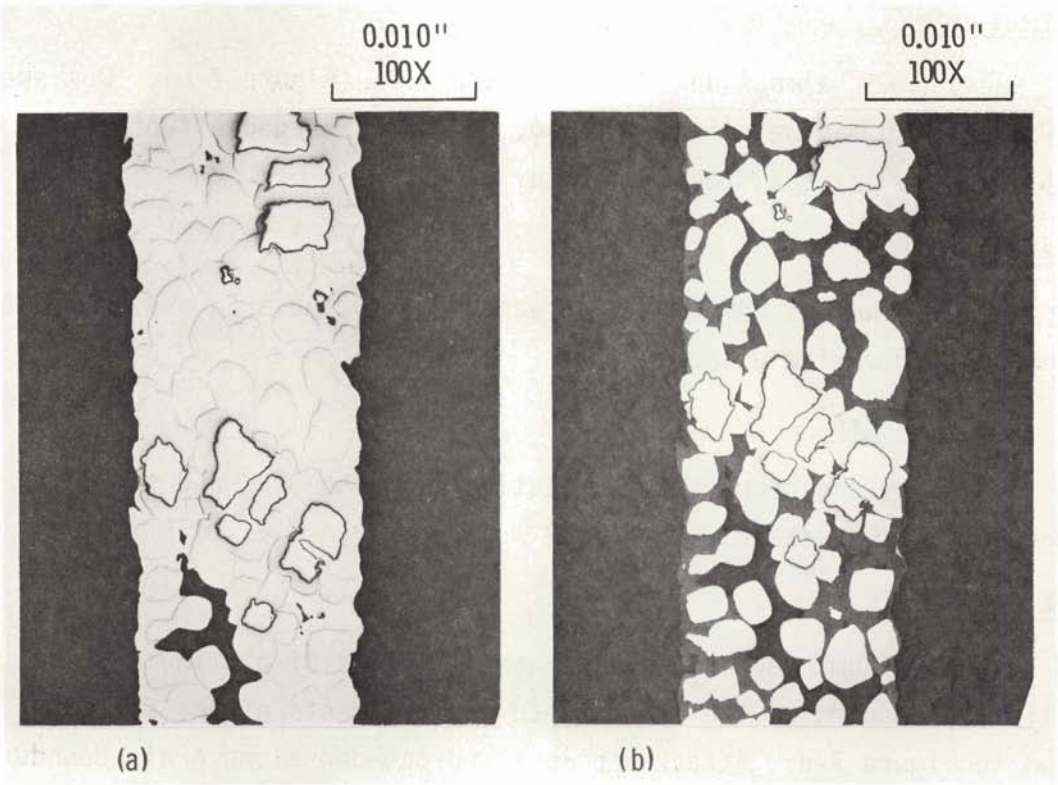

FIGURE 8. Gold Specimens Exposed to SrF_2 at 800°C for 1500 hr

The seawater corrosion tests are being carried out at 23°C using natural seawater with and without aeration. Initial results (up to 320 hr) indicate a very slight but definite weight loss with all the test specimens. The attack is slightly lower with the aerated solution. The average corrosion rates for the first 320 hr exposure are 0.17 mils per year with the aerated solution and 0.21 mils/yr with the unareated solution. At the completion of the tests, which will last 1000 hr; the specimens will be examined metallographically to identify attack mechanisms.

The oxidation tests are being carried out at 600 to 1100°C in 100°C increments. They will also last up to 1000 hr depending on the oxidation rates. The tests have just been started and the initial data are not yet available.

DISTRIBUTION

NO. OF COPIES

OFFSITE

1 ERDA Chicago Patent Attorney
9800 S. Cass Avenue
Argonne, IL 60439

A. A. Churm

1 ERDA Division of Biomedical and Environmental Research
Washington, DC 20545

J. N. Maddox

2 ERDA Division of Production and Materials Management
Washington, DC 20545

F. P. Baranowski
R. W. Ramsey, Jr.

11 ERDA Nuclear Research and Applications Division
Washington, DC 20545

R. T. Carpenter
G. P. Dix
T. J. Dobry, Jr.
N. Goldenberg
A. P. Litman (3)
J. J. Lombardo
W. C. Remini
B. J. Rock
E. J. Wahlquist

1 ERDA Oak Ridge Operations Office
P. O. Box E
Oak Ridge, TN 37830

D. C. Davis, Jr.

3 ERDA Savannah River Operations Office
P. O. Box A
Aiken, SC 29801

R. H. Bass
T. B. Hindman
R. K. Huntoon

NO. OF
COPIES

27 ERDA Technical Information Center

1 Department of the Army
Headquarters, U.S. Army
Facilities Engineering Support Agency
Fort Belvoir, VA 22060

H. Musselman, Technical Director

Electronics and Applied Physics Division
Building 347.3, AERE Harwell
Oxfordshire OX11 ORA
Great Britain

E. H. Cooke-Yarborough

1 General Atomic Company
P. O. Box 81601
San Diego, CA 92138

H. C. Carney

1 General Electric Company MSVD
P. O. Box 8555
Philadelphia, PA 19101

P. E. Brown

1 General Electric Company, Vallecitos Laboratory
P. O. Box 846
Pleasanton, CA 94566

G. E. Robinson

3 Los Alamos Scientific Laboratory
P. 0. Box 1663
Los Alamos, NM 87544

S. E. Bronisz
R. A. Kent
R. N. Mulford

2 Monsanto Research Corporation
Mound Laboratory (ERDA)
Nuclear Operations
P. O. Box 32
Miamisburg, OH 45342

W. T. Cave
R. Dewitt

NO. OF COPIES

1 Naval Nuclear Power Unit
P. O. Box 96
Fort Belvoir, VA 22060

F. E. Rosell

1 Naval Facilities Engineering Command
Nuclear Power Division (FAC04N)
200 Stovall Street
Alexandria, VA 22332

G. E. Krauter

1 Navy Office of the Chief of Naval Operations
Washington, DC 20390

Head, Reactor Branch

4 Holifield National Laboratory
Oak Ridge, TN 37830

R. S. Crouse
J. R. DiStefano
E. Lamb
A. C. Schaffhauser

3 Teledyne Energy Systems
110 W. Timonium Road
Timonium, MD 21093

P. Dick
R. Hannah
P. Vogelberger

1 Westinghouse Astronuclear Laboratory
P. O. Box 10864
Pittsburgh, PA 15236

C. C. Silverstein

ONSITE

3 ERDA Richland Operations

W. A. Burns
W. C. Johnson
P. G. Holsted

NO. OF
COPIES

7 Atlantic Richfield Hanford Company

L. [redacted] Brecke
H. H. Hopkins
R. E. Isaacson
L. M. Knights
C. W. Malody
J. D. Moore
H. P. Shaw

26 Battelle-Northwest

J. W. Bartlett
T. D. Chikalla
M. O. Cloninger
R. L. Dillon
H. T. Fullam (3)
K. M. Harmon
A. J. Haverfield
J. H. Jarrett
R. S. Kemper
R. P. Marshall
R. W. McKee
J. M. Nielsen
R. E. Nightingale
D. E. Olesen
L. D. Perrigo
A. M. Platt
W. E. Sande
J. L. Simmons
H. H. Van Tuyl
R. E. Westerman
Technical Information Files (3)
Technical Publications